RSC Advances

ROYAL SOCIETY OF CHEMISTRY

www.rsc.org/advances

Influence of conformation of monomer on mechanical and tribological properties of thermosetting polyimide

Yanming Wang[a,b], Liming Tao[a], Tingmei Wang[a*], Qihua Wang[a]

[a]State Key Laboratory of Solid Lubrication, Lanzhou Institute of Chemical Physics,

Chinese Academy of Sciences, Lanzhou 730000, China

[b]University of Chinese Academy of Sciences, Beijing 100049, China

Corresponding author: Tingmei Wang; Tel.: +86 0931 4968252 Fax: +86 0931 4968252;

E-mail: wangtin3088@sina.com

Abstract

A series of thermosetting polyimide oligomers with different diamine (isomeride) and same calculated number-average molecular weights (Mn) were synthesized with BPDA (biphenyl-tetracarboxylic acid dianhydride), 4,4'-ODA (4,4'-Oxyidianiline), 3,4'-ODA (3,4'-Oxyidianiline) and 4-PEPA (4-Phenylethynylpathalic anhydride). This paper investigates the effect of configuration of monomer on mechanical, thermal and tribological properties of thermosetting polyimides. Experimental results demonstrate the relationship between molecular configuration and mechanical, thermal and tribological properties. It reveals that as the content of 4,4'-ODA rising, T_g modulus and hardness increases and coefficient of friction (COF) and wear rate (WR) reduce under most conditions. Compared with variations of COFs and WRs of TPIs to velocity or load, it is easy to confirm the major influencing factor under different conditions.

Keywords: configuration, mechanical and tribological properties

1. Introduction

As the important role in polymeric composites, polyimide always attracts many researchers' interest to investigate the properties of polyimide and its composites in many filed, such as: medical area, electronic area, auto motive area and some other industry aspects *etc* [1]. As we all known, imide bond can be formed through condensation between diacid, dianhydride and dihalide with diamine or other methods. The two components of polyimide all have great impact on properties of polyimide. Aromatic polyimides with rigid structure, high strength, thermal stability and excellent anti thermal oxidation, are commonly used for application in engineering, also in tribology, and microelectronics industry. Polyimide composites used as self-lubrication material in engineering often received further attention due to the excellent mechanical and thermal properties. And many papers have discussed about the tribological properties under kinds of conditions [2-4].

Chitsaz-Zadeh[5], JW, Jone[6], Cong[7] and Samyn[8] have done a lot about the chemical structure effect on polyimide tribological performance. And they also proposed some conclusion on the relation between chemical structure and tribological properties. J.W. Jone had proposed that WR showed lowest value for polyimide with flexible linkage. Polyimide with highest friction coefficient showed highest density of polar side groups. Also Chitsza-Zadeh had found that WR were positively correlated with the flexibility of the molecular chains in polyimides. Cong had investigated the tribological difference between thermoplastic and thermosetting polyimide. Also, Samyn had discussed the polyimides performance under high temperature sliding and assessed the tribological performance through the reaction occurred at the sliding interface.

All of the reference except for Cong, is mainly about thermoplastic polyimide. For thermoplastic polyimides with uncrosslink interaction between polymer chains, polymer chains interdigitate through van der Waals force or electron interaction (for polar group). When sliding, polyimide chain at the sliding interface will unloop firstly and rearrange along the sliding direction. So, conclusion about chemical structure effect on polyimide performance is drawn by J.W. Jone, Chitsza-Zadeh and Samyn.

However, for thermosetting polyimides, besides van der Waals force and electron interaction, thermosetting polyimide chains also interdigitate through chemical force [9]. And scission occurred firstly at the sliding interface, which will cause severely fatigue wear and higher COF.

But there is few researches about effect of molecular structure on tribological properties of thermosetting polyimides.

By contrast with thermoplastic polyimide, more factors deeply influenced the manifestation of thermosetting polyimide, such as, molecular weight [10-11], configuration of monomer[12-14], end-capping reagent *etc*. We have investigated the relationship between molecular weight and the tribological performance. A clear conclusion is drawn that significant intrinsic correlation between molecular weight and performance of polyimide. Thermosetting polyimide with the low molecular weight of pre-oligomer presents superior mechanical strength from room to high temperature [10].

Meanwhile, due to the critical role of molecular structure in polymer [5-8], some researches about effect of molecular dynamic movement on polymer performance have been constructed. Lots of simulations have been established to demonstrate and quantize the relation between macroscopy and microscopy. To adjust the desired property, researcher often synthesized polyimide with two or more kinds of diamines and dianhydrides [15-20]. Since the huge impact of synergy of diamine on T_g, solubility, strength and other properties [21-22], it is interesting to exploit the influence of molecular structure on tribological properties of co-polyimides. However, effect of molecule configuration on tribology is not considered yet. It is worthy of exploiting the relation between molecular configuration and tribological properties of polymer. To eliminate the influence of molecular weight, three kinds of thermosetting co-polyimide with the same molecular weight are synthesized with biphenyl-tetracarboxylic acid dianhydride, 4,4'-Oxidianiline (4,4'-ODA) and 3,4'-Oxyidianiline (3,4'-ODA). And 3,4'-ODA is one of the isomers of 4,4'-ODA with its asymmetric structure. The sole difference between these three kinds of polyimide lies in the different ratios of the two kinds of diamines with different conformation. The mechanical strength, micro hardness, tribological properties and their relation under room temperature are discussed in detail.

2. Experiments

2.1Materials

Thermosetting polyimide molding powder was synthesized through the early method [10]. The mole ratio of monomers was listed in table 1. The synthetic process is depicted in fig. 1. And the 3D model structure of BPDA with 4,4'-ODA and 3,4'-ODA are depicted in fig.2.

Table 1 Mole ratio of different monomers

	BPDA	3,4'-ODA	4,4'-ODA	4-PEPA	η [a]/cP
TPI-1	3	4	0	2	19.8
TPI-2	15	4	16	10	27.3
TPI-3	3	0	4	2	29.2

a μ: measured in DMF at a concentration of 15 wt.% at 30 ℃.

BPDA (biphenyl-tetracarboxylic acid dianhydride), 4-phenylethylphthalic anhydride (4-PEPA), 4,4'-ODA (4,4'-Oxyidianiline) and 3,4'-ODA (3,4'-Oxyidianiline) was purchased from Changzhou Sunlight Pharmaceutical Co., Ltd. 1-Methyl-2-pyrrolidinone (NMP) was dried with molecular sieve and distilled in vacuum then stored in sealed flask and purchased from Sinopharm Chemical Reagent Co., Ltd.

2.2 Methods and measurements

Differential scanning calorimetry (DSC) was performed on a NETZSCH DSC-200F3 thermal analyzer in nitrogen. Thermal gravimetric analysis (TGA) was performed on a NETZSCH-STA449F3 series thermal analysis system at a heating rate of 10 ℃/min in nitrogen at a flow rate of 50 cm^3/ min.

Nano-indentation tests were performed on a TI-950 triboindenter (Hysitron, American) using a Berkovich diamond indenter. After contacting with the surface, the indenter was stuck into the friction specimens with a constant strain rate of 0.05 s^{-1} until 2000 nm of depth was reached, and then withdrawn from the surface with the same rate as loading. At least ten indents were performed on each specimen and the average value was finally adopted. The hardness was calculated by the Oliver and Pharr method.

The bending strength of the specimens was determined in a three-point test machine with a span of 30mm and crosshead speed of 2 mm/min. The specimens were 50mm×8mm×3mm and the test surface was 50mm×8 mm. The specific bending strength (σ_f) of the specimen was calculated from Eq. (1).

$$\sigma_f = \frac{3P.l}{2b.h^2} MPa \qquad \text{Eq. (1)}$$

Where P is the maximum load (N), l is the span length (mm), b is the width of specimen (mm), h

is the thickness of the specimen (mm).

Worn surface of TPI and transfer film was characterized by SEM (JSM-5600LV). The worn

surfaces were gold coated using the ion sputtering method.

Before the tribological test, the worn surface of the specimen was polished with

metallographical sand paper to make sure that all specimen surfaces were testing under the same

roughness concentration (Ra=0.1μm).

2.3 Preparation of PI specimens

The composites were fabricated by means of hot press molding technique. The molding

condition was determined through DSC data. Before hot press molding, the composite powders

were pulverized. The powders were compressed and heated to 375 ℃ (the temperature is

determined by DSC in characteristics) and held at 20 MPa for 1 h to allow full compression and

curing. At the end of each run of compression sintering, the resulting specimens were cooled with

the stove in air, cut into pre-set sizes for tribological (2×2×18 mm) and mechanical tests.

2.4 Friction test

The tribological tests were conducted on a ball (GCr15, 3 mm) on disc wear testing machine

(CSEM-THT07-135). The contact schematic diagram of the frictional couple is shown in fig. 3.

The wear rate was calculated with the following equation [10]. Tribological tests are conducted

under the loads of 1 N, 5 N, 10 N, 20 N. And every specimen is tested under the given loads with

three different velocities of 0.05 m/s, 0.1 m/s and 0.5 m/s, respectively. The sliding distance is 300

m except for the test under 20N/0.5m/s (1000 m). Wear rate is calculated from Eq.2.

$$\Delta V = [\frac{\pi(\frac{R}{2})^2}{180} arcsin\frac{b}{R} - \frac{b\sqrt{(\frac{R}{2})^2 - (b/2)^2}}{2}]\pi d \qquad Eq.2$$

$$K = \frac{\Delta V}{PL}$$

ΔV, Volume wear rate (mm3); R: Couple diameter (3.000 mm); b: Circle width (μm); d: Circle

diameter (10 mm); K: Wear (mm^3/N·m); P: Load (N); L: Sliding distance (m).

3. Characteristics

3.1 Thermal properties

From the first DSC scans of TPI oligomers in fig. 4, it is obvious to see that there is no

crystallization produced during the synthesis process. And the exothermic peak indicated that crosslink reactions of the three TPI oligomers started at approximately 350 ℃, 358 ℃ and 366 ℃, respectively. Meantime, the oligomer with more rigid diamine (4,4'-ODA) reacted at higher temperature (with more energy to trigger the reaction). This is attributed to the close stack of the polymer chain in TPI-3, which greatly hindered the movement of polymer molecular. So, the molding temperature is set at 375 ℃.

Fig.5 shows infrared spectrum of TPI after hot-pressing technique. It is obvious that the ethynyl C≡C absorption band at 2213 cm^{-1} disappears in the TPI specimens, which demonstrates the accomplishment of thermal curing reaction of 4-PEPA [15]. It can be concluded that all the TPI specimens are all already well cross-linked based on FT-IR spectrum. Theoretically, it should be noted that under the same molding process parameters, the TPIs with different molecular configuration have sligthly different crosslink density, which can be ignored. Polyimide with more asymmetric diamine corresponds to a little higher crosslink density. Therefore, the difference of mechanical and tribological properties between the TPIs in this work should be considered as a result of synthesized effects of molecular configuration and crosslink density. However, we proposed that diamines with different configurations dominated the properties in this paper.

Consistent with our speculation, molecular configuration have little influence on the initial decomposition temperature in nitrogen (See Fig. 6). TPI-1, TPI-2 and TPI-3 exhibited excellent thermal stability with the onset decomposition temperatures at 540 ℃, 544 ℃ and 549 ℃, respectively. By contrast, it has huge impact on stack of polymer chain, which influences the residual weight retention. As we can see, TPI-1 with more asymmetric diamine in polymer chain has the highest residual weight retention at 1000 ℃, which is consistent with the result in reference [23].

Meanwhile, molecular configuration also affects the glass transition temperature (T_g) substantially (See fig. 7). Thermosetting polyimide with more asymmetric 3,4'-ODA presents lower T_g, and the corresponding T_g sequence is, TPI-1 < TPI-2 < TPI-3. Besides, loss tangent (tanσ), which closely relates with molecular structure of polymer and molecular interaction, also presents higher value with the higher 3,4'-ODA content in polymer chain at the glass transition temperature. The more asymmetric units in molecular chain of polymer, the stronger of the molecular interaction, which results in higher value of tanσ and different peak shapes at the glass

7

transition temperature.

3.2 Mechanical properties

Meanwhile, hardness and Young's modulus of TPIs show higher value with higher content of 4,4'-ODA in polymer chain (See fig. 8a). With the same crosslink density, symmetrical monomer will result in well stack in polymer chains when molding. So hardness increases with less in 3,4'-ODA content in polyimide. Young's modulus of TPIs also presents the similar trend.

Effect of monomer configuration on mechanical property is investigated through bending strength and modulus test (See fig. 8b). It is obvious that polyimide with more 4,4'-ODA presents higher bending strength and modulus, which resulted from the symmetric and rigid structure.

3.3 Friction behavior

Average COFs of TPIs are depicted in fig. 9 under different velocities and loads. It is obvious that COFs of TPIs decrease with load rising under different velocities. Meanwhile, as the rise of 3,4'-ODA content in TPI, TPI shows higher COF under most condition except for COF of TPI-1 under 1 N and 0.5 m/s. COF of TPI-2 which consists of both diamines of 3,4'-ODA and 4,4'-ODA, presents the middle COF between TPI-1 and TPI-3, except for the condition mentioned above. The higher COF of TPI-1 results from the entanglement of the polyimide chains due to the more asymmetric molecular configuration of 3,4'-ODA. Moreover, friction heat plays a more important role on TPI-1 with lower T_g than polymer with higher T_g (TPI-2, 3), as the velocity rise from 0.05 m/s to 0.5m/s. And this can be clearly seen from the performance of TPI-1 under 20N and 0.5m/s (See fig. 10). The sharp drop of COF predicts the variation of polymer at the friction interface, which affects the friction process at the interface. And this can be proved by the SEM of the worn surface (See fig. 11c) and lumpy transfer film (See fig. 10), which is attributed to the friction heat under such harsh condition [24].

Contrast to the monotone decrease in COF of TPI-1, WR of TPI-1 decreases from 1 N to 5 N under different velocities (See fig.12). And WR rises with the increase in load from 5 N to 20 N. Under lower load, friction heat produced by velocity dominates the test process. WR of TPI-1 decreases with rise in velocity. And the difference of TPI-1 between 1 N and 5 N became small, from 3.17×10^{-4}, 2.6×10^{-4} to 8.8×10^{-6}, respectively for 0.05 m/s, 0.1 m/s and 0.5 m/s. Besides, WR of TPI-1 also declined with velocity rising. However, with the load increase, WR escalates rapidly under all velocities, which apparently indicates the huge dependence of TPI-1 on load, especially

under high velocity (0.5 m/s).

Different with TPI-1, WR of TPI-2 decreases with load rising only under 0.0 5m/s and 0.1 m/s. However, under 0.5 m/s. WR of TPI-2 decreases from 1N to 5 N, then increases from 5N to 20 N. meanwhile, WR decreases with velocity increasing. As for TPI-3, WR decreases with load or velocity rising under every velocities and load conditions. This is attributed to the high T_g, which enables polymer maintain its strength under the same condition.

4. Discussion

4.1 Effect of monomer configuration on COF

To qualitatively evaluate the effect of molecular configuration on tribological properties of TPIs, variations of COFs and WRs of TPIs to velocity and load is presented in fig. 13, 14, 15 and 16. The dependence of material on operating velocity or load is rated as low if variation is as close to zero as possible or undulations in the curve are minimal or in other words the curve should tend to be straight line parallel to the x-axis [25]. Meanwhile, if the value is plus it means COF decreased with rise of velocity or load. On the contrary, it means COF increased with rise of velocity or load.

Fig. 13 depicts variation of COF against load at two speed transitions (transition one:from 0.05 m/s to 0.1 m/s and transition two: from 0.1 m/s to 0.5 m/s). It is obvious that TPI-1 has little dependence on load at the first speed transition corresponding to the small variation in fig. 13a. However, at the second speed transition, COF of TPI-1 decreases vastly (See fig. 13b). The high value of COF variation of TPI-1 indicates the huge impact of velocity on TPI-1 under different loads. Meanwhile, the relatively straight curves of TPI at the two speed transitions predict that TPI-1 has little dependence on load.

Different with the high variation in the first speed transition and low variation in the second speed transition of TPI-1, variation of TPI-2 shows opposite trend. Compared to performances of TPI-1 and 2, it can be drawn that monomer configuration has great impact on the friction properties of polymer. For TPI-1 composed with one kind of diamine (3,4'-ODA see table 1), polyimide chains intertwined each other, which hinders rearrangement and movement of molecular at the contact surface. Only enough energy can conquer its internal friction or entanglements (physical and chemical crosslink) in polymer chain, such as high velocity and load. Under high load and velocity, more energy input will produce more friction heat, which can affect

9

polymers' mechanical strength at the sliding interface and further friction coefficients. And COF variation of TPI-1 presents more stable at the first speed transition than at the second transition. So, it is easy to understand the high value of variation of COF for TPI-1 at the second speed transition.

TPI-3 presents more stable in the whole process except for at 1 N. Under most conditions, COF variation of TPI-3 always maintains a relatively low value. Meanwhile, combined with the smooth worn surface in fig.11, it is easy to predicts that COF of TPI-3 can easily reach a steady state under low load (corresponding to low energy input), which is attributed to the symmetric molecular structure in polymer theoretically. Equally, TPI-2 composed with two kinds of diamines presents higher COF variation at the first speed transition and lower COF variation at the second transition. At the first speed transition, the less energy input can conquer the entanglements in polymer chain of TPI-2. So, the low variation value of TPI-2 occurred at the first speed transition, compared to the high variation value of TPI-2 at the second speed transition.

To evaluate the dependence of TPIs on load and velocity comprehensively, difference of COFs against load as a function of velocity is plotted in fig. 14. From fig.14a it can be deduced that the big variations in COF of TPI-2 and TPI-3 indicate the easy shear for TPI-2 and TPI-3 compared to TPI-1. This can be attributed to the different interaction in polymer chain, which is consistent with conclusion drawn from the analysis of fig. 12. Meanwhile, as the load increasing, the variation of TPI-2 and TPI-3 shows small value compared with that of TPI-1 (See fig. 14b). And this also can be contributed to the strong interaction in molecular chain of TPI-1 than that in TPI-2 or TPI-3. For TPI-2 and TPI-3, the higher variations in the first load transition compared to that in the second load transition also implys the easy shear of TPI-2 and TPI-3 under lower load. As the load rising, in fig. 14c, the nearly straight line predicts the stability of COF of TPI-3 under higher load as a function of velocity.

4.2 Effect of monomer configuration on WR

In generally, WR of TPI-1 with more 3,4'-ODA has great dependence on load and velocity. This can also be demonstrated in SEM picture (See fig. 11-a,b,c). The apparent cracks on worn surface of TPI-1 under 20 N and 0.1 m/s diminished on worn surface of TPI-1 under 20 N and 0.5 m/s and 10 N and 0.5 m/s. Trace of melt of polymer can be found in SEM picture of 20 N,10 N and 0.5 m/s. Meanwhile, the sudden drop of the friction of TPI-1 under 20 N and 0.5 m/s is the most direct evident of change of physical state of polymer at the sliding interface.

WR of TPI-2 shows different trend under different velocities as a function of load. From the worn surface morphology in fig.11-d,e,f, it is easy to understand the variation. Under lower velocity, worn surface of TPI-2 presents severe cracks. Under lower velocity and load, the synergy of load and velocity is not enough to support the movement of molecular at the contact surface. More cracks occurred on the worn surface (See fig. 11-d). Under the suitable velocity (5N/0.1m/s, See fig.12-b, TPI-2,), the input energy promotes the movement of polymer chain at the sliding interface without causing huge crack of polymer (See fig. 11-e). However, under higher load and velocity (20 N, 0.5 m/s), scallops caused by peeling off appears on the worn surface again (See fig.11-f), which corresponds to the higher wear at 0.5 m/s.

WR of TPI-3 has little dependence on load and velocity under the test conditions in our paper. Under low load and velocity or high load and velocity, worn surface of TPI-3 all present relatively smooth surface morphology (See fig. 11-g,h,i).

To qualitatively assess the effect of load and velocity on WR of TPIs, the difference between velocity and load are poltted as a function of load or velocity, respectively in fig.15 and fig. 16. Fig. 15 depicts WR variations of TPIs under two speed transitions from 0.05 m/s to 0.1 m/s (first transition in fig. 15a) and 0.1 m/s to 0.5 m/s (second transition in fig. 15b) as a function of load. The higher WR variations of TPI-1 and TPI-2 indicate velocity has great influence on wear performances on TPI-1 and TPI-2. WR variation of TPI-1 decreased from 1 N to 5 N firstly and then increased beyond 5 N. This also indicates load has important impact on WR of TPI-1 at the first speed transition. Also this predicts the great impact of load on WR of TPI-1 at the first speed transition. WR variations of TPI-2 and 3 decreased and stabilized at the first speed transition as load rising, which implies load has less influence on WR of TPI-2 and 3, especially beyond 5 N. Compared with TPI-2 and 3, TPI-1 relies greatly on load at the first speed transition when load is beyond 5 N. The rise of load leads to increase in contact area, which has close relation with friction and wear [26]. For TPI-3, load and velocity has little effect on their WRs when load is beyond 5 N, in the first speed transition. Meanwhile, TPI-3 presents more stable in the second speed transition

At the second speed transition, WR variation of TPI-1 presents the similar trend with that in the first speed transition. Under high load and speed, friction heat has serious influence on polymer molecular morphology at the contact surface, which results in soft or melt that can

11

accelerate wear of TPI-1 (See fig. 11 c). Combining with the worn morphologies in fig. 11 b and c, it is easy to figure out the reason that TPI-1 shows such a variation at 20 N under the higher speed transition. As for TPI-2 and 3, there is only small variation at the high speed transition, which indicates the less dependence on test condition and its stability of TPI-2 and 3. All the difference can be attributed to the different mole ratio of diamine in polymer chain. TPI-1 with asymmetric 3,4'-ODA resulted in loose chain stack which exhibits lower T_g, modulus and hardness, compared with TPI-2 and 3. Lower T_g results in sharp drop of COF under high speed and load, which is own to friction heat (See fig. 10). For TPIs, lower modulus, hardness and bending strength resulted from loose stack in polyimide chain, which play a crucial role on tribological performances.

Fig. 16 depicts variations of WRs of TPIs against load as a function of velocity. At the first load transition, variations of WR of TPIs decrease as increase in velocity and are all above zero. This means WRs decrease as load reach to 5 N. Meanwhile, speed also has great impact on WR of TPI-1. This can be attributed to the strong entanglement of polyimide chain of TPI-1, which hindered the rearrangement of molecular chain and resulted in poor anti-wear of polymer and higher COF [23].

At the second load transition, the plus WR variation value of TPI-3 predicts that WR decreases as load rising, compared with the minus WR variation value of TPI-1 and TPI-2. This implies the better anti-wear property of TPI-3 under the same test condition. Significantly, variation values of TPI-1 and TPI-2 are below zero. Meanwhile, the big absolute variation value of TPI-1 compared to TPI-2 indicates the worse anti-wear property of TPI-1.

At the third load transition, variations of WR present more stable for TPI-2 and TPI-3. The relatively straight curves in the second and third load transition predict the stability of WR to velocity. Meanwhile, the minus value means the increase in WR as load rising. But for TPI-1, contrast to variation in first load transition, WR increases as increase in load especially under lower velocity (0.05m/s and 0.1 m/s). Compared with the different performances of TPI-1, TPI-2 and TPI-3 in fig. 16, it is easy to conclude that variations of WR of TPIs have a close relation with polymer composition. With higher content of 4,4'-ODA in polymer chain, the lower absolute variation value of WR implies the stability of TPI under the test conditions. So, combined with the anti-wear performance in fig.12, a conclusion can be drawn that TPI-3 with higher 4,4'-ODA content in polyimide composition presents better anti-wear property than TPI-1 and TPI-2.

12

5. Conclusion

Three kinds of thermosetting co-polyimide with the same crosslink density and molecular weight were synthesized by BPDA (biphenyl-tetracarboxylic acid dianhydride), 4-PEPA, and different mole ratios of 4,4'-ODA (4,4'-Oxyidianiline) and 3,4'-ODA (3,4'-Oxyidianiline). Some mechanical, thermal and tribological properties were examined in our paper. And there exist some intrinsic relation between molecular configuration and macro performance. Conclusions are drawn as follows:

1. With the higher 4,4'-ODA content in polymer chain, T_g, modulus, hardness and bending strength of TPI presents higher value due to the more symmetric structure in polymer molecular which results in a more close stack of polymer chain.

2. With the higher 4,4'-ODA content in polymer chain, COF decreased under three kinds of velocity at different loads except for TPI-1 at 1N, 0.5 m/s. High COF of TPI-1 can be ascribed to the asymmetric diamine (3,4'-ODA), which results in serious entanglement and internal friction in polymer chain, which hinders movement in friction test and leads to high value of COF. Equally, under 0.1 m/s and 0.5 m/s, WR of TPIs presents the similar trend, respectively.

3. Through variations of COFs and WRs, we can qualitatively concluded that configuration of monomer has important effect on polymer's performance. For example, COF of TPI-1 depends greatly on speed (See fig. 13 and fig. 14, the second speed transition), however WR of TPI-1 depends on speed and load simultaneously (See fig. 15 and fig. 16). Contrast to TPI-1, tribological perperties of TPI-3 appears more stable and immune to load and velocity under most conditions.

6 Acknowledge

Reference

[1] Sroog CE. Polyimides. *Progress in Polymer Science* 199; **16**: 561-694.

[2] Kim J, Im H, Cho MH. Tribological performance of fluorinated polyimide-based nanocomposite coatings reinforced with PMMA-grafted-MWCNT. *Wear* 2011; **271**: 1029-38.

[3] Wang QH, Zhang XR, Pei XQ. Study on the synergistic effect of carbon fiber and graphite and nanoparticle on the friction and wear behavior of polyimide composites. *Materials & Design* 2010; **31**: 3761-8 (2010)

[4] Samyn P, Quintelier J, Schoukens G, De Baets P. The sliding behaviour of sintered and thermoplastic polyimides investigated by thermal and Raman spectroscopic measurements. *Wear* 2008; **264**:869-76.

[5] Chitsaz-Zadeh MR, Eiss NS. Friction and wear of polyimide thin films. *Wear* 1986; **110**: 359-368.

[6] Jone JW, Eiss Ns. Effect of chemical structure on the friction and wear of polyimide thin films. ACS Symposium Series 1985; **287:**, 135-148.

[7]Cong PH, Li TS, Liu XJ. Effect of temperature on the friction and wear properties of a crosslinked and a linear polyimide. *Acta Polymerica Sinica* 1998; **5:** 556-561.

[8]Samyn P, Schoukens G, Verpoort F, Craenenbroeck J. Friction and Wear Mechanisms of Sintered and Thermoplastic Polyimides under Adhesive Sliding. *Macromolecular Materials and Engineering* 2007; **292:** 523-556.

[9]Maeda N, Chen N, Tirrell M, Israelachvili JN. Adhesion and friction mechanisms of polymer-on-polymer surfaces. *Science* 2002; **297:** 379-382.

[10] Smith JG, Connell, JW, Hergenrother, PM. The effect of Phenylethynyl Terminated Imide Oligomer Molecular Weight on the Properties of Composites. *Journal of Composite Materials* 2000; **34**: 614-628.

[11]Connell, JW, Smith, JG, Hergenrother, PM and Rommel, ML. Neat resin adhesive and composite properties of reactive additive/PETI-5 blends. *High performance polymers* 2000; **12**: 323-333.

[12] Yokota R, Yamamoto S, S. Sawaguchi YT, Hasegawa M, Yamaguchi H, *et al*. Molecular design of heat resistant polyimides having excellent processability and high glass transition temperature. *High Performance Polymers* 2001; **13**: S61-72.

[13] Masatoshi H, Sensui N, Shindo Y, and Yokota R. Structure and Properties of Novel Asymmetric Biphenyl Type Polyimides. Homo- and Copolymers and Blends, *Macromolecules* 1999; **32:** 387-396.

[14] Ogasawara T, Yokota R, Toshitaka W, Aoi T, Goto J. Processing and properties of carbon fiber/Triple-A polyimide composites fabricated from imide oligomer dry prepreg. *Composites: Part A , applied science and manufacturing* 2007; **38**: 1296-1303.

[15] Wang YM, Wang TM, Wang QH. Effect of molecular weight on tribological properties of thermosetting polyimide under high temperature. *Tribology International* 2014; **78:** 47-59.

[16] Qiu W, Zhang K, Li FS, Zhang K, Koros WJ. Gas Separation Performance of Carbon Molecular Sieve Membranes Based on 6-FDA-*m*PDA/DABA(3:2) Polyimide. *Chemsuschem* 2014; **7:** 1186-94.

[17] Maya EM, Garcia-Yoldi I, Lozano AE, de la Campa JG, de Abajo J. Synthesis, Characterization, and Gas Separation Properties of Novel Copolyimides Containing Adamantyl Ester Pendant Groups. *Macromolecules* 2014; **44:** 2780-90.

[18] Huertas RM, Tena A, Lozano AE, de Abajo J, de la Campa JG, Maya EM. Thermal degradation of crosslinked copolyimide membranes to obtain productive gas separation membranes. *Polymer Degradation and Stability* 2013; **98:** 743-50.

[19] Li W, Guo X, Fang J. Synthesis and properties of sulfonated polyimide-polybenzimidazole copolymers as proton exchange membranes. *Journal of Materials Science* 2014; **49:** 2745-53.

[20] Kins CF, Sengupta E, Kaltbeitzel A, Wagner M, Lieberwirth I, Spiess HW, et al. Morphological Anisotropy and Proton Conduction in Multiblock Copolyimide Electrolyte Membranes. *Macromolecules* 2014; **47:** 2645-58.

[21] Wang W, Zhou H, Chen D, Wu M, Liu Y, Chen C. Preparations and Properties of a High Performance Semicrystalline Copolyimide and Composites Reinforced with Glass Fiber. *Journal of Applied Polymer Science* 2014; **131:** 40410.

[22] Li TS, Tian JS, Huang T, Huang ZY, Wang HY, Lu RG, et al. Tribological Behaviors of Fluorinated Polyimides at Different Temperatures. *Journal of Macromolecular Science Part B-Physics* 2011; **50:** 860-70.

[23] Huang T, Liu P, Lu R, Huang Z, Chen H, Li T. Modification of polyetherimide by phenylethynyl terminated agent for improved tribological, macro- and micro-mechanical properties. *Wear* 2012; **292-293:** 25-32.

[24] Samyn P, De Baets P, Schoukens G. Influence of Internal Lubricants (PTFE and Silicon Oil) in Short Carbon Fibre-Reinforced Polyimide Composites on Performance Properties. *Tribology Letters* 2009; **36:** 135-46.

[25] Satapathy BK, Bijwe J. Composite friction materials based on organic fibres: Sensitivity of friction and wear to operating variables. *Composites Part A: Applied Science and Manufacturing* 2006; **37:** 1557-67.

[26] Aoike T, Yokoyama D, Uehara H, Yamanobe T, Komoto T. Tribology of ultra-high molecular weight polyethylene disks molded at different temperatures. *Wear* 2007; **262:** 742-8.
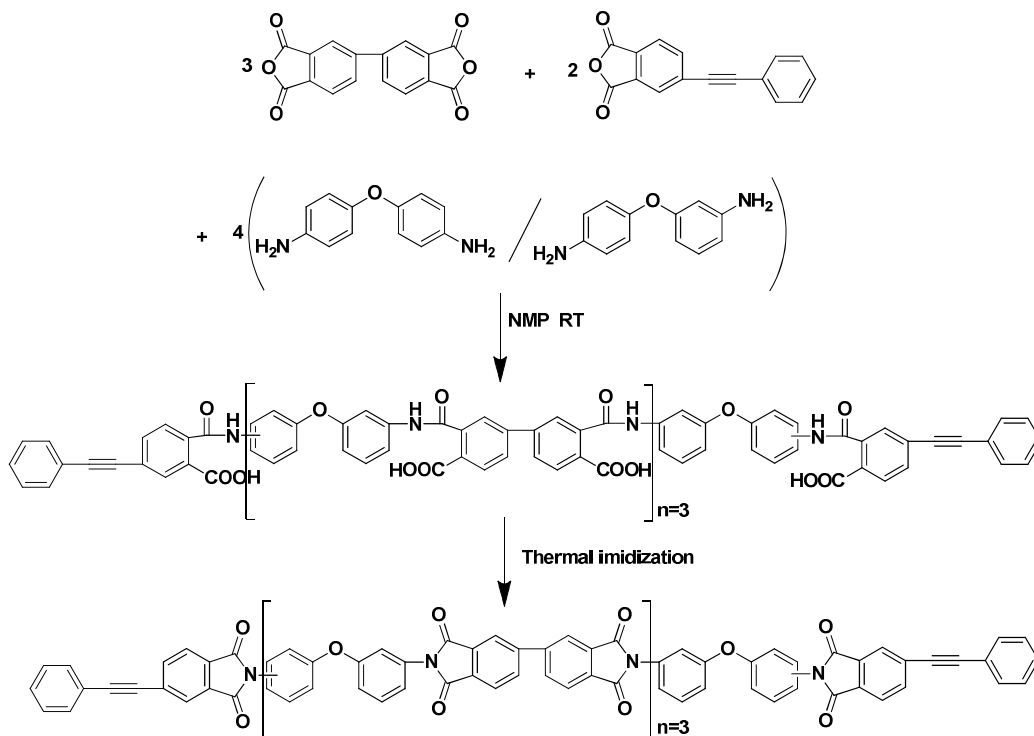
Fig.1 Synthesis of polyimide oligomers with different mole ratios of diamine
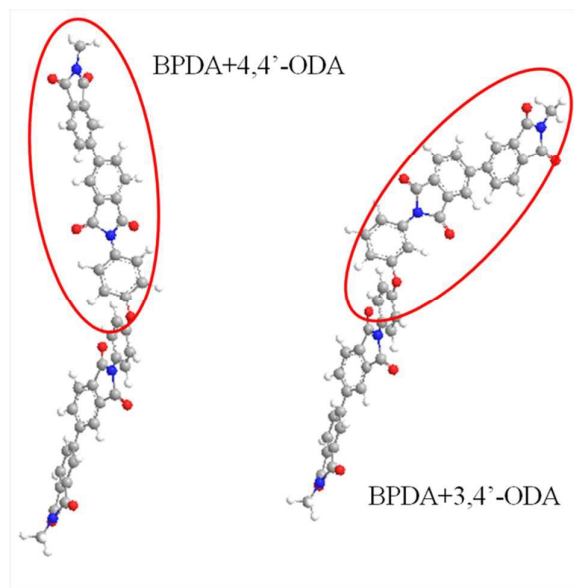
Fig.2 The 3D model molecular structure of BPDA with 4,4'-ODA and 3,4'-ODA
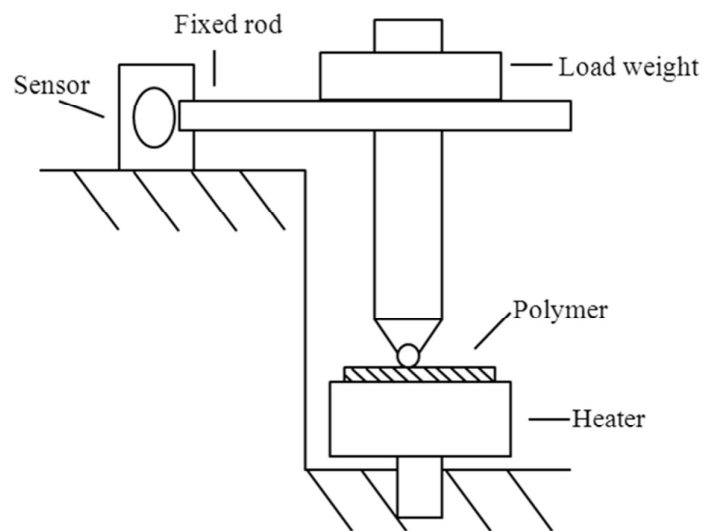
Fig. 3. Schematic diagram of the contact configuration of the reciprocating friction
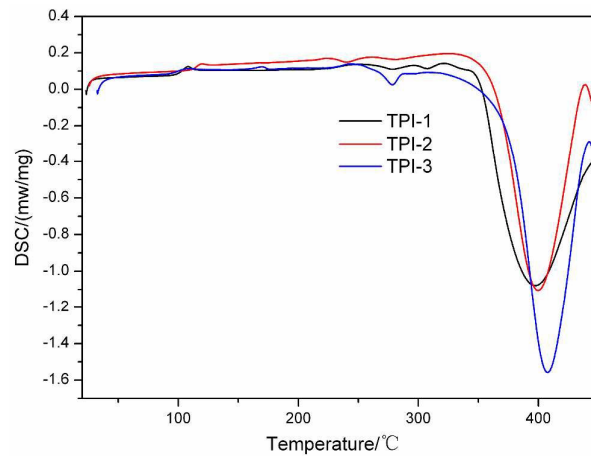
Fig. 4 The first DSC scan of TPI oligomers in nitrogen
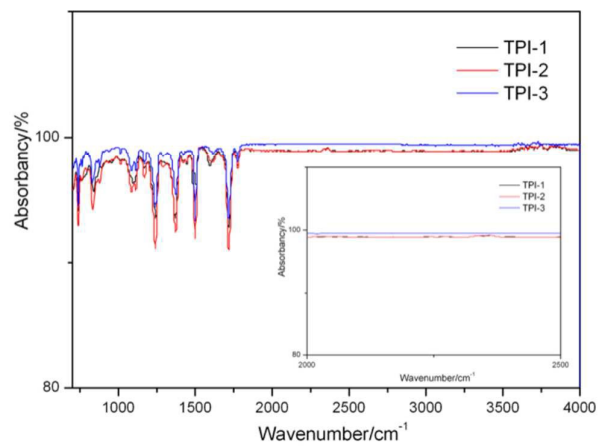
Fig.5 Attenuated total reflectance IR spectra of TPI-1,2,3
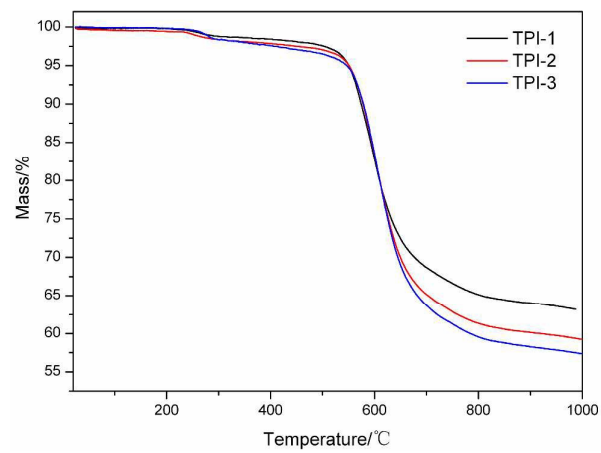
Fig. 6 Weight loss of the three kinds of polyimide in nitrogen
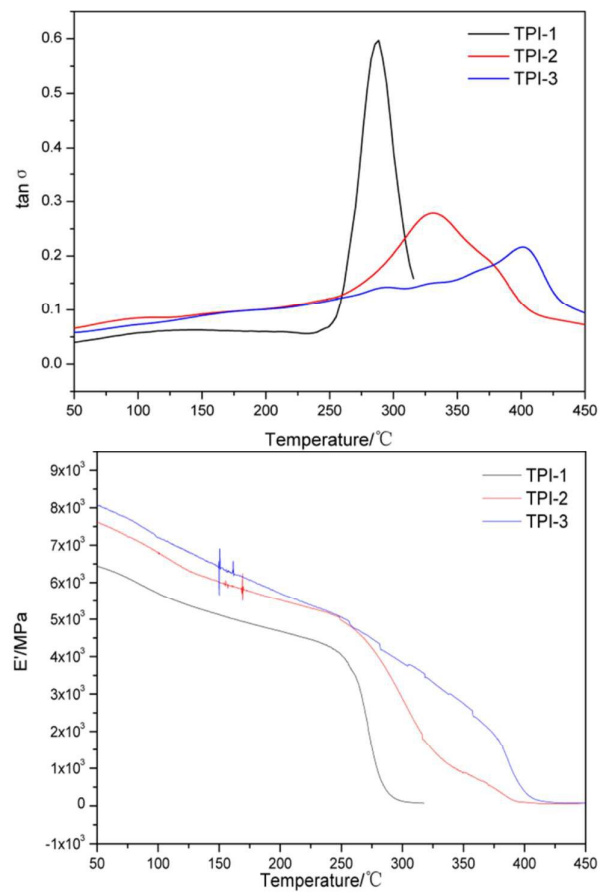
Fig. 7 DMA of thermosetting polyimides
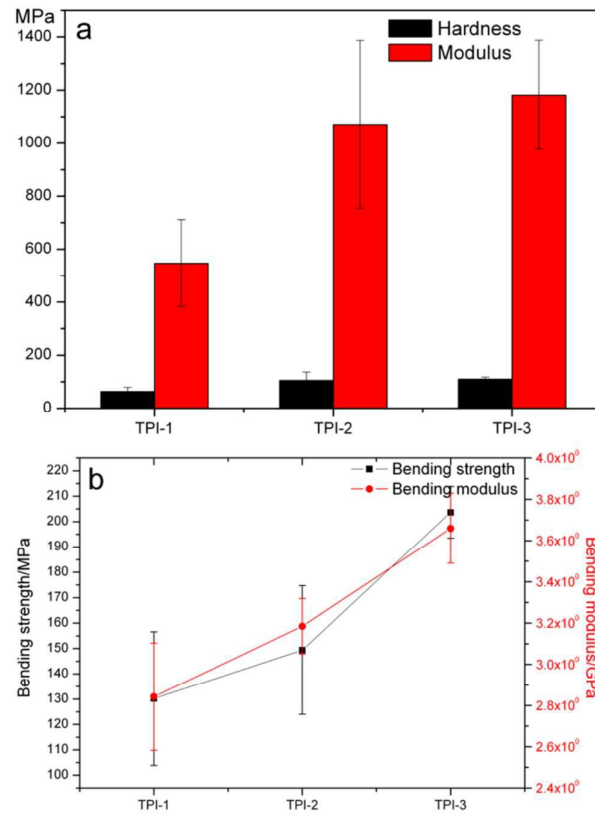
Fig. 8 Mechanical properties of TPI-1, TPI-2 and TPI-3,

a: Hardness and Elasticity modulus

b:Bending strength and modulus
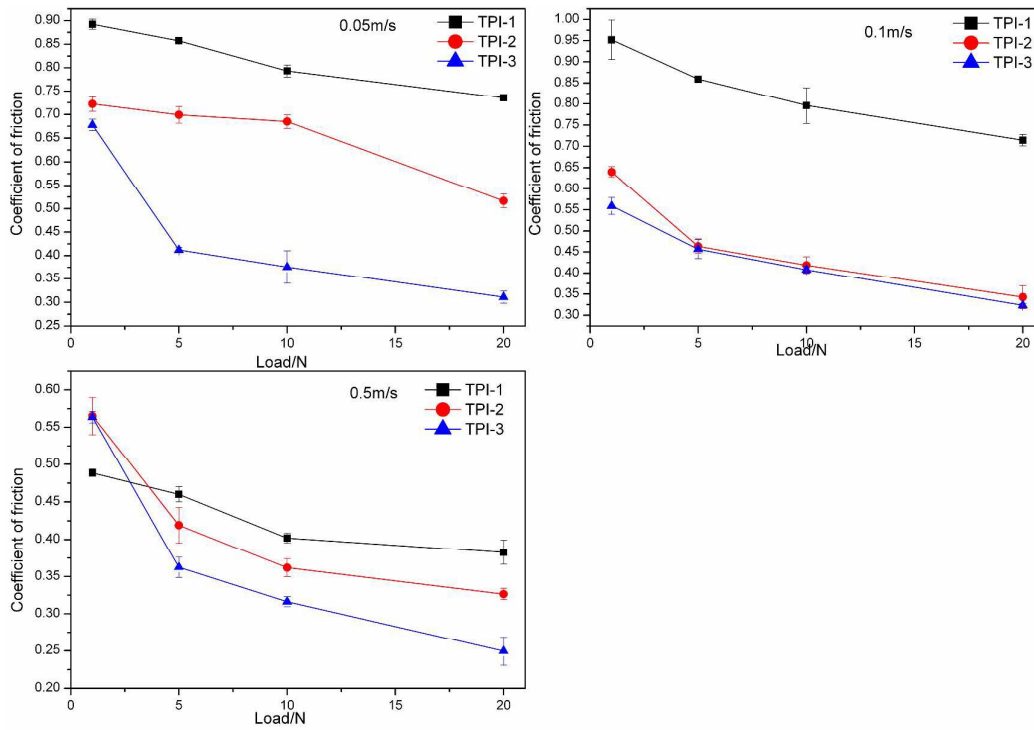
Fig. 9 Coefficient of friction of TPI-1, TPI-2 and TPI-3 under different velocities as a function of

load
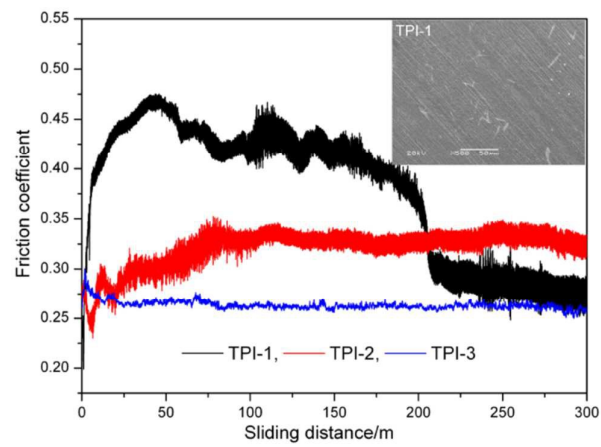
Fig. 10 Sliding course of TPI-1, 2 and 3 under 20N, 0.5m/s and transfer film of TPI-1
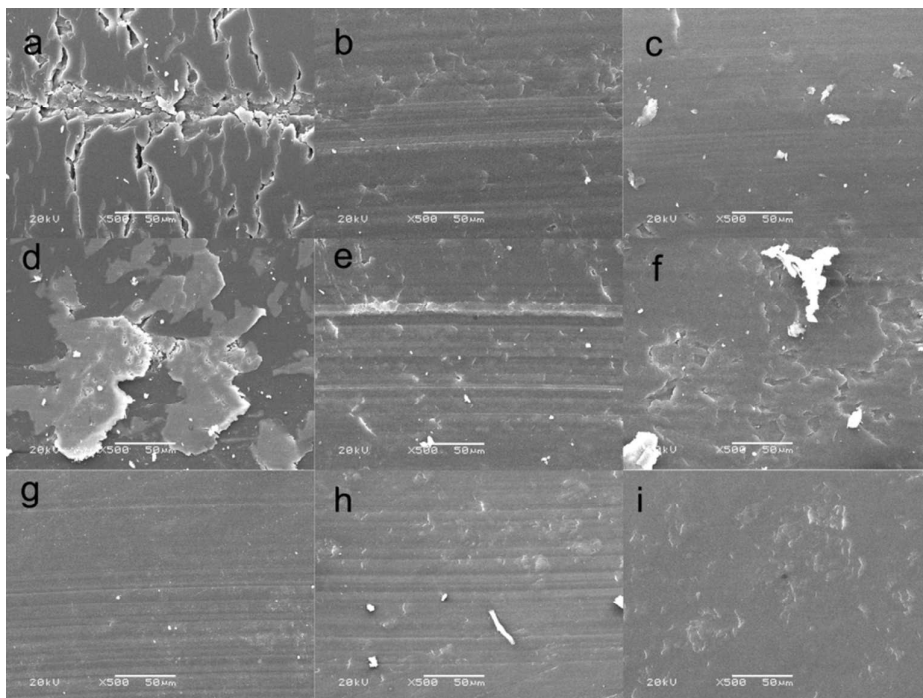
Fig.11 Worn surface of TPI-1,2,3 under different conditions,
TPI-1; a, b, c; 20N/0.1m/s, 10N/0.5m/s, 20N/0.5m/s,
TPI-2; a, b, c; 5N/0.05m/s, 5N/0.1m/s, 20N/0.5m/s,
TPI-3; a, b, c; 1N/0.05m/s, 5N/0.1m/s, 20N/0.5m/s,
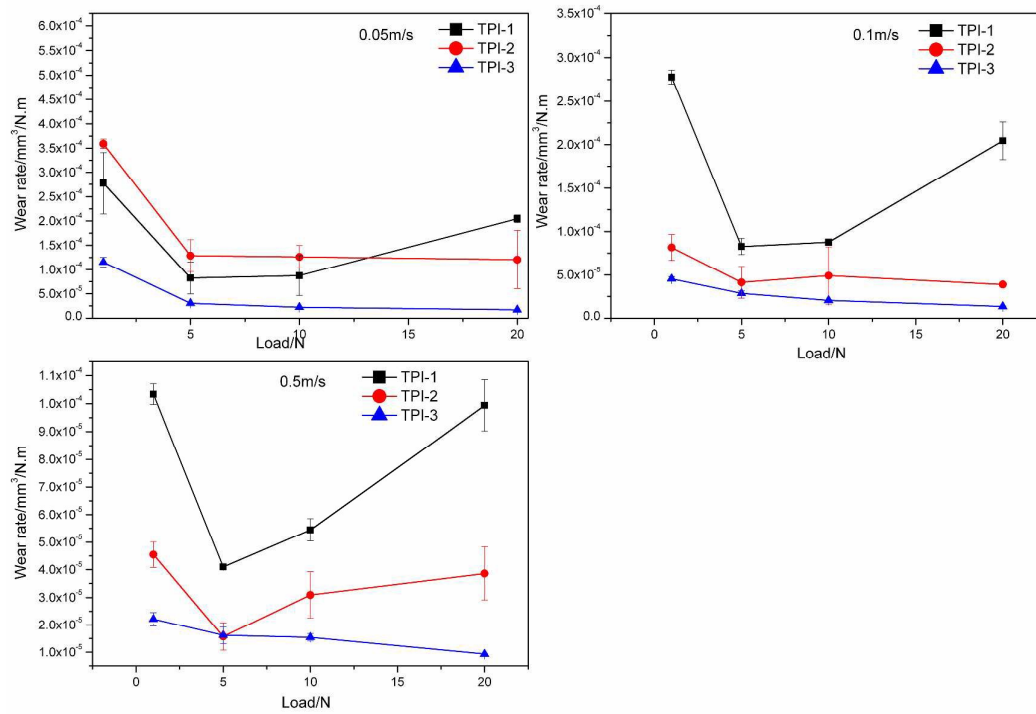
Fig. 12 Wear rate of TPI-1, TPI-2 and TPI-3 under different velocities as a function of load
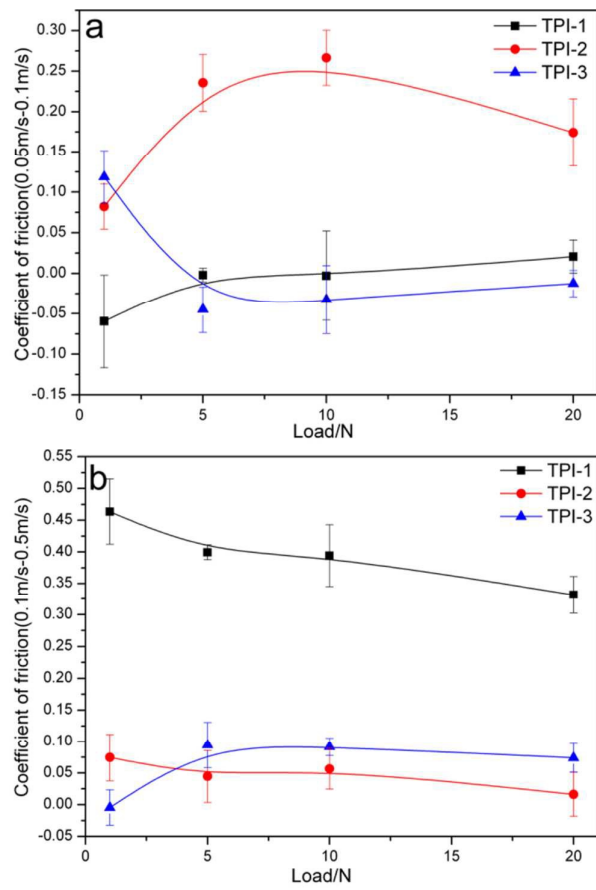
Fig. 13 Difference value of COF to velocity,

a: Δ_{COF}(0.05m/s-0.1m/s); b: Δ_{COF}(0.1m/s-0.5m/s)
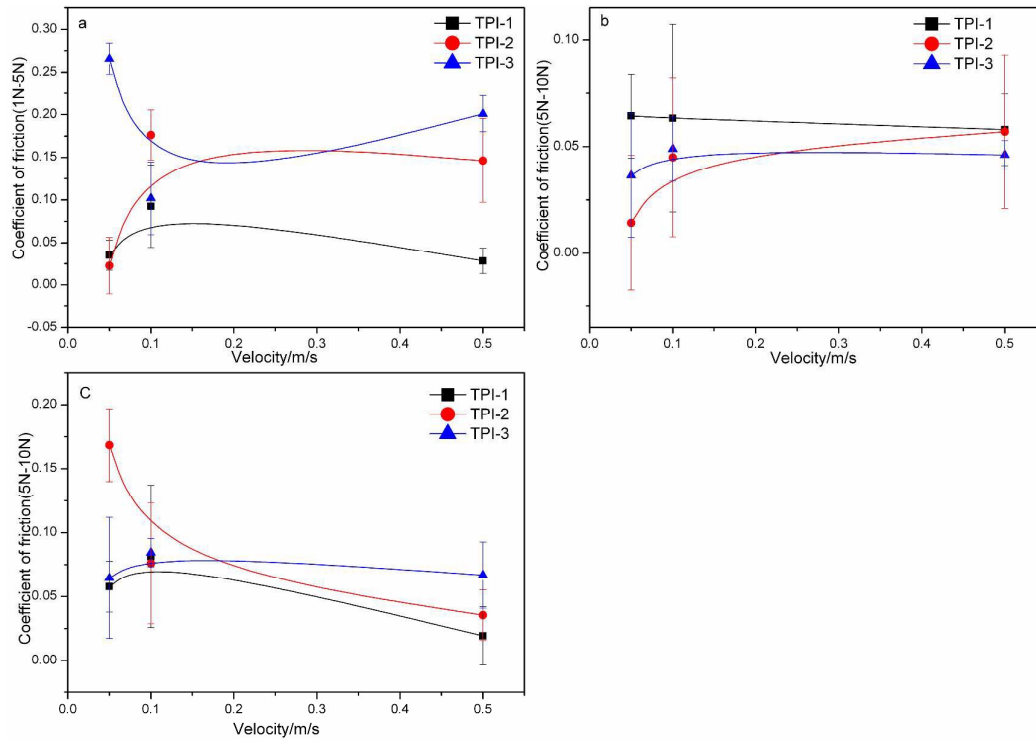
Fig. 14 Difference value of coefficient of friction to load, a: Δ_{COF}(1 N-5 N), b: Δ_{COF}(5 N-10 N), c: Δ_{COF}(10 N-20 N)
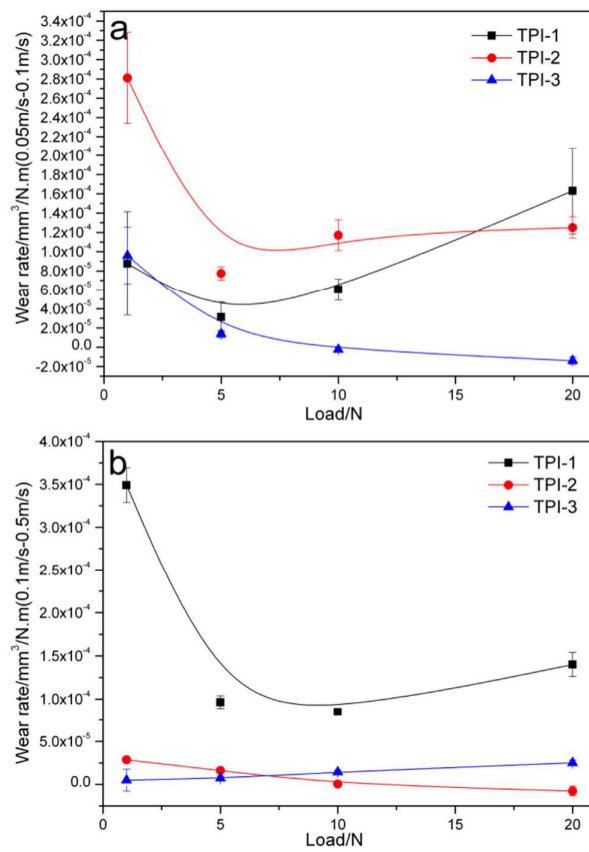
Fig. 15 Difference value of WR to velocity

a: Δ_{WR}(0.05m/s-0.1m/s); b: Δ_{WR}(0.1m/s-0.5m/s)
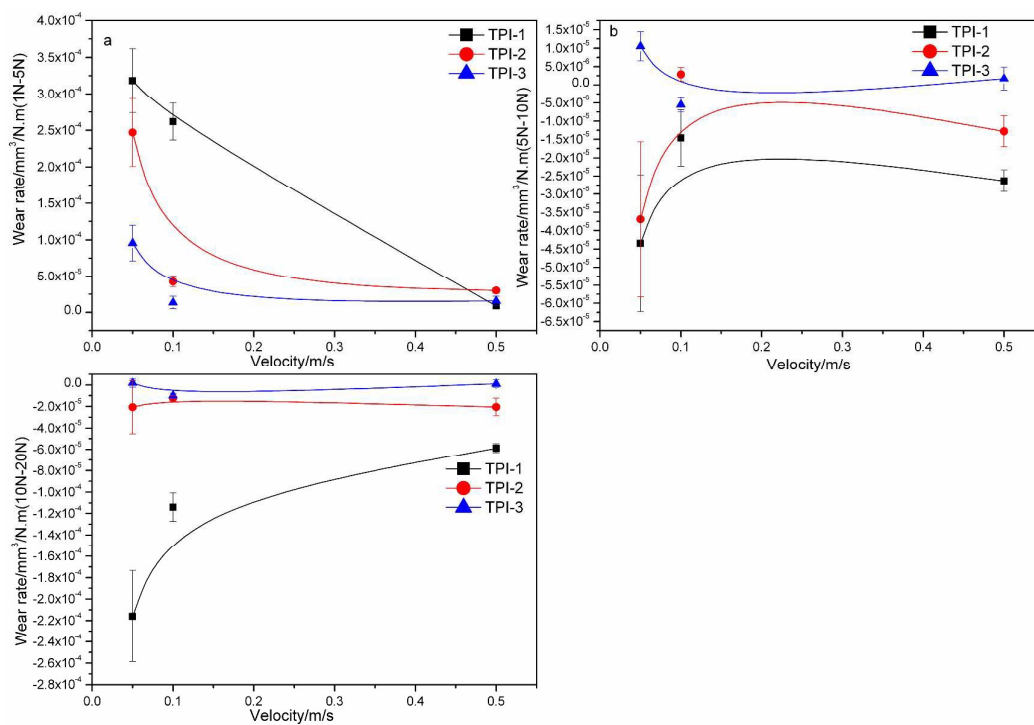
Fig. 16 Difference value of wear rate to load, a: Δ_{WR}(1 N-5 N), b: Δ_{WR}(5 N-10 N),

c: Δ_{WR}(10 N-20 N)

40x20mm (600 x 600 DPI)